Rijksuniversiteit Groningen

Bachelor Thesis

Radio jets in young stellar objects

Author:
I.Eissa

Supervisor:
Floris.v.d.Tak

Abstract

Jets of young stellar objects have shown to be either thermal jets associated with free-free emission or non-thermal jets as a result of synchrotron emission. Our goal is to differentiate between thermal and non-thermal jets by looking for trends through their protostellar physical parameters. We use radio continuum observations of the Karl G. Jansky Very Large Array done by Gould's Belt Survey to study the spectral indices and flux densities of 706 young stellar objects in the Orion and Taurus-Auriga regions. We also compare our findings with literature values for the magnetic field strength in order to understand the environment of the jets. We find that non-thermal jets have a stronger magnetic field reaching values up to 10^{-1} G, two orders of magnitude higher than thermal jets. Mass-loss rates acquired in the outflows shows a linear trend for the optically thick jets linked with free-free emission while non-thermal jets mass outflow do not vary much. The magnetic field in non-thermal jets is powerful enough to deny any instabilities that might affect the mass-loss rate.

Contents

1 Introduction

Dense cloud regions are considered to be the main site of star formation where hydrogen is in molecular form (Motte, Bontemps, & Louvet, 2018). Numerical modeling and theoretical proposed mechanisms helped us understand observations of the birth of young stars where two scenarios of accretion have been proposed (Tan et al., 2014). In case of monolithic core accretion, the range of star-masses is wide depending on the density of the cloud and cluster mass function where the condensed gas in the core collapse under its own gravity after failing to sustain the thermal pressure, leading to an accretion process mediated by the central disk. On the other hand, competitive accretion is based on gas being chaotically drawn into a starless core, where eventually the massive protostar will be at the center of the clump and roaming around it are lower-mass stars that were created through the ambient gas circling the massive star. During the accretion processes in both cases, one of the main feedback mechanisms that help us study the properties of the sources is outflows (Shu et al., 1987; Tan et al., 2014).

Outflows are crucial for star formation since they allow the continuation of the accretion process by removing the excess angular momentum (Hawley et al., 2015). For an isolated-low-mass star region, observing the bipolar outflows is the only available feedback we can detect (Elmegreen & Scalo, 2004). However, massive stars feedback can be its initial mass function or disruption it does to its surroundings allowing us to study the object and predict its mass. The origin of the outflows themselves is not completely understood yet due to the high extinction present in the dense environment of star forming regions. (Blandford & Payne, 1982) proposed earlier on the importance of magnetic field in these conditions.

Protostellar outflows are best observed at radio wavelengths, since the extinction by dust is minimal in this range (Obonyo et al., 2019).The most used tracers to study the radio knots are CO emission and Herbig-Haro(HH) objects. HH objects are the product of the shocked outflow originating from the protostar interacting with the surrounding medium (Schwartz, 1983),creating optical emission in low excitation lines(e.g [OI] and [SII]). Outflow tracers can be high-velocity emission in the radio frequency range of H_2O masers (Kavak et al., 2021; Rodriguez et al., 1980). Both HH objects and H_2O masers have been linked to the outflows of stars through their proper motions in terms of tangential velocities (Arce et al., 2007), and an observational tracer is dependent on the evolutionary stage of the outflow source.

Observations at radio frequencies showed that free-free emission found in thermal jets is not the only emission that can be detected through the radio jets. Feigelson and Montmerle (1985) detected non-thermal emission in the jets coming from highly energetic electrons emitting synchrotron radiation. Consequently, at present, the gould's belt survey confirmed 1041 sources of radio jets that could be either thermal or non-thermal jetsacross 4 star formation regions of different initial mass functions (Dzib et al., 2013; S. A. Dzib et al., 2015; Kounkel et al., 2014; Ortiz-Leó n et al., 2015).

The distinction between thermal and non-thermal protostellar bipolar outflows is yet to be found. Thermal jets are dominated by free-free emission which is produced through the deflection of a high energy electron by a local electric field made by a H^+ nucleus (Draine, 2011). The spectral index of the jets ($S_\nu \propto \nu^\alpha$) (Reynolds, 1986), where S_ν is the flux density of the radio jets, ν is the frequency used to observe the corresponding flux and α is the spectral index of the source calculated by the relation mentioned. Positive spectral indices are expected from radio jets dominated by free-free emission, depending on the spectral index, the regime can be either optically thin or thick , Purser

et al. (2016) defined the optically thick region to have a spectral index of $1 < \alpha \leq 2$ and optically thin at $-0.1 \leq \alpha \leq 1$. On the other hand,negative spectral indices are accompanied by the result of having accelerated electrons from shocks in the vicinity of a strong magnetic field existing in non-thermal jets, emitting synchrotron radiation (Bordovitsyn & Ternov, 1999). Non-thermal jets are in the optically thin regime but are hard to observe due to the optically free-free emission regime surrounding it (Anglada et al., 2018).

The goal of this research is to be able to classify and reason the thermal and non-thermal radio jets found in YSOs. To be able to do that, we aim to analyse star formation regions through the use of Gould's Belts Survey database. Gould's Belts Survey is a project that concentrated on observing radio jets of YSOs found in star formation regions around the Gould's Belt (Dunham et al., 2015). We will search for correlation between the young star's physical properties and having a thermal or non-thermal radio jet emission.

2 Theoretical background

2.1 Magnetic field effect on outflows

Protostars of low and intermediate mass are known to have an accretion disk roaming around its core, these disks are the supplier of gas for the young star in the center. Donati et al. (2005) proved the presence of a strong magnetic field of value 1kG in the inner region of the disk in order to sustain the high accretion rate($10^{-4} M_{\odot} \mathrm{yr}^{-1}$ the protostars have. Consequently, this observation indirectly assisted the theory of magnetized jet proposed by Blandford and Payne (1982) and was later confirmed by (Carrasco-Gonzalez et al., 2010) who used the Karl G. Janksy Very Large Array(VLA) to find the first observational evidence of a magnetised jet in HH 80-81 using radio continuum emission.

Originally magnetic fields were not thought to be involved in the outflow process since winds from the accretion disk were suggested to be the main drivers of the jets (Pudritz & Norman, 1983), stating hydromagnetic winds carry the angular momentum and energy outwards in the form of jets. The reasoning was not further approved due to high resolution spectro-imaging technology which revealed the rotation of the collimated jets in addition to having a complex structure in terms of velocities which cannot be solely done by disk wind (Bacciotti et al., 2003; Pudritz, Ouyed, Fendt, & Brandenburg, 2006). Moreover the ejected momentum was orders of magnitude higher than what the radiation pressure could afford (Lada, 1985). Blandford and Payne (1982) theory of magnetohydrodynamics(MHD) was solidified by these conclusions, the spiral-shaped magnetic field around the accretion disk, allowing the protostar to shed the additional angular momentum and gravitational potential energy by ejecting bipolar outflows. Recently Kee et al. (2016) suggested outflow creation by stellar wind of OB stars being passed through UV radiation line's scattering, however there have not been any tests about this proposition since it is quite new. Low-mass Class 0 YSOs do not have the gravitatoonal potential energy to launch outflows since Class 0 are in an early stage of accreting where the envelope mass is bigger than core mass. Quasispherical winds are the limit for Class 0 stars in terms of outflows (Bally, 2016; Barsony, 1994)

Magnetised accretion disks experience magneto-rotational instability(MRI) due to the difference in angular velocity between between the inner and the outer region of the accretion disk resulting in turbulence in the MHD which affects the transported angular momentum to the jets (Balbus & Hawley, 1991). Magnetic field is always accompanied by a magnetic flux, in this case the flux's field lines are acting perpendicularly on the accretion disk (Kigure & Shibata, 2005). The resulting force surpasses the gravitational pull applied from the core resulting in a vertical ejection of accelerated ionised material into the ambient medium. The blasting of hot-ionised-high velocity gas into a cooler-slower medium creates Kelvin-Helmholtz(KH) instability in addition to shock waves leading to high velocity shock-compressed layer as shown in Figure 1.

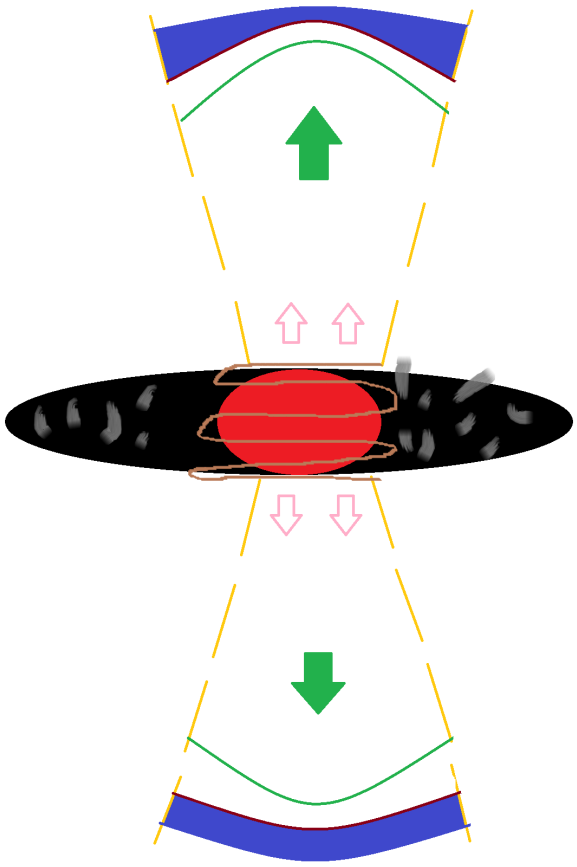

Figure 1: A rough sketch of the outflow process inspired by Bally (2016), the spirally lines(brown) represent the magnetic field around the inner core of the star(red) pushing materials perpendicular to the accretion disk and in a parallel direction with the magnetic flux arrows(pink). The ejected ionised gas (green) led by shock front interacts with the ambient medium (blue) representing the molecular outflow tracers. Making the shape of a collimated jet bounded by the cavity walls(yellow).

The simultaneous events triggered due to MHD and the instabilities show how unstable and chaotic the vicinity of a protostar is. However, it is not efficient enough for MHD and disk winds are not sufficient to create collimated jets (Begelman, 1998). Toroidal component of the magnetic field plays a role in applying the tension needed to direct the outflows into a lobe. The presence of the toroidal field line surfaces in the alfvén region where the kinetic energy density of the flow is less than the magnetic field energy density. The structure of the lobes depend on multiple physical parameters of young stellar object such as core luminosity, age of the source and mass accretion rate. It also depends on the observational tracer that was used, Rodríguez-Kamenetzky et al. (2020) used radio continuum high resolution images (0.″12x0.″09) to analyse massive young stellar objects(MYSO), through their free-free emission. The morphologies of the jets ranged up to $\approx$ 0.1 arcsecond in addition to calculating the proper motions of the thermal jets on the course of 22 years to be in the range of $\approx$112 $\sim$118 km s^{-1}.

2.2 Thermal jets

Thermal free-free emission was thought to be the only tracer at radio wavelengths to study the radio jets, which resulted in Reynolds (1986) modeling the mass outflow rate, injection radius and jet velocity for positive spectral indices. Rodriguez et al. (1989) though, detected negative spectral index which suggested non-thermal jets. The history for observations of radio jet source clearly shows that thermal jets are the more common type of jets in young-low mass stars based on the VLA observations of young star candidates Anglada et al. (2018). Thermal jets are dominated by free-free emission which have a positive spectral index, meaning that the flux density increases with frequency. These jets tend to be optically thick, making harder to measure their physical parameters. Additionally, two different Taurus region surveys indicated the low variability of flux density in thermal jets and their polarization to be linear (S. A. Dzib et al. (2015);Cohen and Bieging (1986);Anglada et al. (2018)).

2.3 Non-thermal jets

Relativistic jets are observed in large scale jets from Active Galactic Nuclei extending up Mpc, where shocks are the main producer of relativistic electrons (Blandford & Ostriker, 1978). However, in our case where we focus on young stars, electrons are not as easily accelerated as in AGNs. Synchrotron radiation in AGN has been detected at low radio frequencies as a result of high energy electrons being around a magnetic field (Mohan, Vig, & Mandal, 2022). Synchrotron radiation results in negative spectral indices found in powerful radio knots and the first observed evidence were by Reid et al. (1995) using the H_2O masers outflow and Carrasco-Gonzalez et al. (2010) became the first to evaluate the magnetic field of a magnetized jet, the collimated jets of HH 80-81 was linearly polarized had a magnetic field of ~ 0.2 mG . Non-thermal jets have high variability in terms of the flux density(>50%) due to changes in direction of the ejection and the degree of collimation in the outflows (Reipurth & Bally, 2001).

Class I are more evolved YSOs than Class 0 as they build a star core and the envelope mass drastically decreases. Synchroton radiation are expected from magnetically active Class I YSOs, however the optically thick environment of free-free emission complicates the detection of synchrotron radiation. One possibility is for the source to have a convective rotationally driven layer that could supply the magnetic activity we detect (Dzib et al., 2010).

The degree of polarization ranges between 10 % to 30% of the total emission detected (Carrasco-Gonzalez et al., 2010). The existence of synchrotron radiation allows the likelihood of having a circular polarization, the conversion from linear polarization to circular polarization could happen when having low energy electrons being around relativistic electrons and the presence of either magnetic field resulting in MHD or Faraday's rotation which we can expect in non-thermal jets due to the relativistic particles. Circular polarization is generally found in synchrotron emission regimes, where its production can be through MHD causing MRI which results in turbulences. This allows the conversion from linearly polarized to circularly polarized.

3 Methods

3.1 Observations

Recently, jets studies have been focusing on individual massive protostars since a higher angular resolution is obtained with large arrays such as VLA and Atacama Large Millimeter Array(ALMA), having a resolution of sub-arcsecond. Purser et al. (2016),Purser et al. (2021) and Vig et al. (2017) analysed massive young stellar objects and classified 64 sources to have ionized jets. However, in the case of our research, mass amount of YSOs are our main target in order to come out with reliable correlations and properties. The Gould's Belt Survey probed two dense clouds and their data contained a large diversity in the spectral index calculated. In Subsection 3.2, we will go through the data we used from the survey catalogs of Orion and Taurus-Auriga. regions(Dzib et al., 2013; S. A. Dzib et al., 2015; Kounkel et al., 2014)

3.2 Gould's Belt Survey

Gould's Belt Survey focused on star formation regions around the Gould belt, the survey used the VLA to observe the regions of Orion and Taurus-Auriga at radio frequency bands of 4.5GHz and 7.5GHz to obtain the flux density,spectral index, variability and the errors accompanying the parameters mentioned (Dunham et al., 2015). Unlike the 7.5GHz, the 4.5GHz datasets for the sources were the main usage in this project due to having more sources in the band.

For the orion cloud, 374 sources were detected where 148 of them were previously identified as young stellar objects(YSO), while the Taurus-Auriga complex observed a total 603 sources in the 4.5GHz band, with already known 196 YSOs. The other sources were recorded as either extragalactic objects or a star within the Milky Way. Figure 2 shows the amount of radio sources detected jets in both regions, leaving us with a completed set of data for 706 sources.

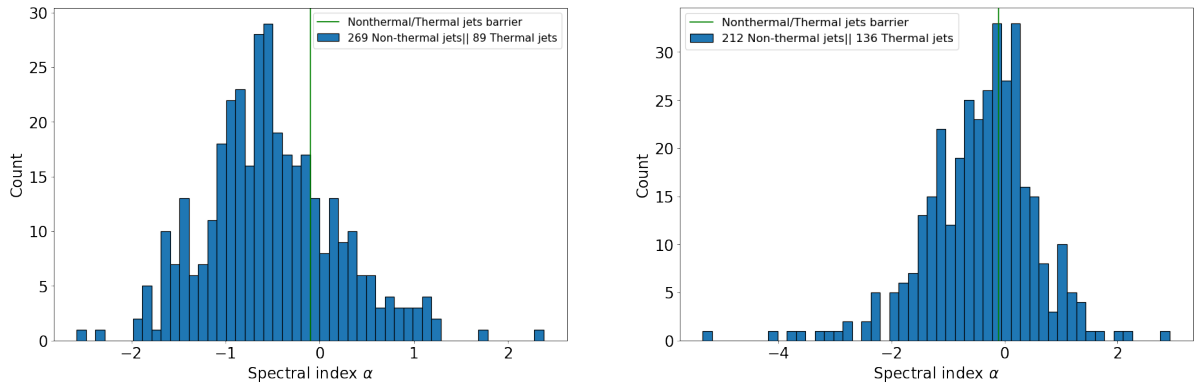

(a) **(b)**

Figure 2: Distribution for the radio sources in terms of their spectral indices for Taurus-Auriga region(a) and Orion region(b) where a green vertical line at $\alpha = -0.1$ separates the non-thermal and thermal jets.

3.3 Physical Parameters

3.3.1 Mass outflow rate

Mass outflow rate is a primary parameter for a forming protostar that could tell us the outflow velocities and the morphology of the outflow.
However, to be able to calculate the outflow rate, we used Purser et al. (2016) and Reynolds (1986) categorization of the jet spectra, where we used the spectral index to approximate the model of the jet. For $0.4 \leq \alpha < 0.8$, a "standard" spherical model jet is assumed, in the case of $\alpha \geq 0.8$, a recombining jet model is assigned and for $\alpha < 0.4$ a "standard" collimated model was given. We used Purser et al. (2016) equation for the mass-loss rate given by:

$$\dot{M}_{\rm Jet} = \frac{9.38 \times 10^{-6} v_8 \, \mu \, S_{\rm mJy}^{3/4} \, d_{\rm kpc}^{3/2} \, \theta_0^{3/4}}{x_0 \, \nu_{10}^{\alpha} \, \nu_{m10}^{0.45-\frac{3\alpha}{4}} \, T_4^{0.075} (\sin i)^{1/4} F^{3/4}} \tag{1}$$

$v_8 \equiv v/10^8 {\rm cms}^{-1}$ is the ionized gas expansion velocity and assumed to be 500 km s^{-1}, μ is the average particle mass taken to have a value of 1, α is the spectral index, d_{kpc} is the distance to the source, in this case we assume all the sources in Orion complex to be at a distance of 414 $\pm$ 7 pc (Menten, K. M. et al., 2007) and the Taurus-Auriga cloud sources to be at 137$\pm$ 20 pc (Torres et al., 2007), $S_{\rm mJy}$ is the integrated flux density, ν_{10} is the frequency band used for the observation, ν_{m10} is the turnover frequency where it's value is assumed to be 50GHz for $\alpha > 0$ since it becomes optically thick because of free-free emission. On the other hand, in case of $\alpha < 0$ we took the turnover frequency to be the smallest observation frequency band that was used in the observations, in this case it was set to be 4.5GHz. Moreover, θ_0 is the deconvolved opening angle of the outflow, F is the term based on Table 1 in Reynolds (1986), i is the angle of inclination taken to be 60°(Purser et al., 2016; Sanna et al., 2016), x_0 is the ionisation fraction assumed to be 1 since we are calculating the ionized mass and T_4 is the electron temperature in the medium which is assumed to be 10^4K for these regions.

3.3.2 Magnetic field

Synchrotron radiation emission depends on the strength of the magnetic field around it, therefore estimating the magnetic field for all the radio jets we acquired is essential in order to potentially find a relation between non-thermal jets and the magnetic field. For a standard energy distribution of electrons, we made use of the equipartition of energy between the magnetic field and the relativistic particles,which as a result allow us to estimate the magnetic field through (Vig et al., 2017):

$$\begin{aligned}\left(\frac{B_{\rm eq}}{\rm gauss}\right) = 5.69 \times 10^{-5} &\left[\frac{1+K}{\eta(\sin\phi)^{3/2}(\alpha+1/2)}\left(\frac{\rm arcsec^2}{\theta_{\rm x}\theta_{\rm y}}\right)\right]^{2/7} \\ &\times \left[\left(\frac{\rm kpc}{s}\right)\left(\frac{F_{\rm o}}{\rm Jy}\right)\frac{\left(\nu_2^{\alpha+1/2}-\nu_1^{\alpha+1/2}\right)}{\nu_{\rm o}^{\alpha}(\alpha+1/2)}\right]^{2/7}\end{aligned} \tag{2}$$

Where F_o is the radio flux density at the observed frequency ν_o, s is the distance to the source, $\theta_{\rm x}$ and $\theta_{\rm y}$ are the beam sizes for the major and minor axis, respectively.The arithmetic mean value of the beam sizes for the VLA observations for the Taurus-Auriga region and was also applied to the orion region since Kounkel et al. (2014) did not mention the synthesized beam size they recorded for their sources. α is the spectral index determined for the source, K is the ratio of energy between heavy relativistic protons and electrons, η is a filling factor because of the beam, ϕ is the angle

between our observations line-of-sight and the magnetic field of the outflow, which is taken to be $\sim$ 34 °(Vig et al., 2017). Higher and lower cutoff frequencies were assigned to be ν_2 and ν_1, respectively and their values were assumed by Miley (1980) to be ν_1= 0.001GHz and ν_2=100GHz . The only limitation for this approximation is that, we cannot mathematically work out the magnetic field for sources with spectral index of value $\alpha = -0.5$, therefore we had to eliminate these sources for this calculation.

3.3.3 Bolometric luminosity

Flux density and the distance to the source were used to calculate the bolometric luminosity of the source which is an essential parameter in our research. We wanted to test the correlation between the mass outflow rate and the bolometric luminosity due to the positive relation expected between them (Bally, 2016). We approximate the bolometric luminosity of the sources at a frequency of 4.5GHz byAnglada et al. (2018):

$$\left(\frac{S_v d^2}{\mathrm{mJykpc^2}}\right) = 10^{-1.90\pm0.07}\left(\frac{L_{\mathrm{bol}}}{L_\odot}\right)^{0.59\pm0.03} \tag{3}$$

Where the radio continuum luminosity is empirically correlated with the bolometric luminosity of the source.

3.3.4 Momentum

Energy supplied to the ambient medium through the shocks in the outflow can be estimated from the amount of momentum found in the lobes, the more core mass the YSO has, the more energy it has to offer for the outflows. Therefore we calculated the momentum through its correlation with the radio luminosity in the centimeter continuum using the equation (Anglada et al., 1992; Anglada et al., 2018; Cabrit & Bertout, 1992):

$$\left(\frac{S_V d^2}{\mathrm{mJykpc^2}}\right) = 10^{2.97\pm0.27}\left(\frac{\dot{P}}{M_\odot \mathrm{yr}^{-1}\ \mathrm{km\ s}^{-1}}\right)^{1.02\pm0.08} \tag{4}$$

In which $S_\nu d^2$ is the radio continuum luminosity at frequency of 4.5GHz observed as direct relation for the momentum. The main reason for calculating the momentum rate is to observe its effect on the magnetic field in the lobes

4 Results

Here we present our findings regarding the parameters of the outflow, investigating any correlations that could be found that may help to understand the behaviour of the jets in terms of their physical parameters. Expecting from the relations to have a direct contrast between the type of jets in order to help the science community with further research projects on the observations of outflows.

4.1 Spectral index vs. Magnetic field

Considering that the magnetic field is the main factor affecting synchrotron emission, it was essential to find out the dependence of the magnetic field in terms of YSOs properties, therefore the spectral index is the perfect candidate to understand the strength of the magnetic field.

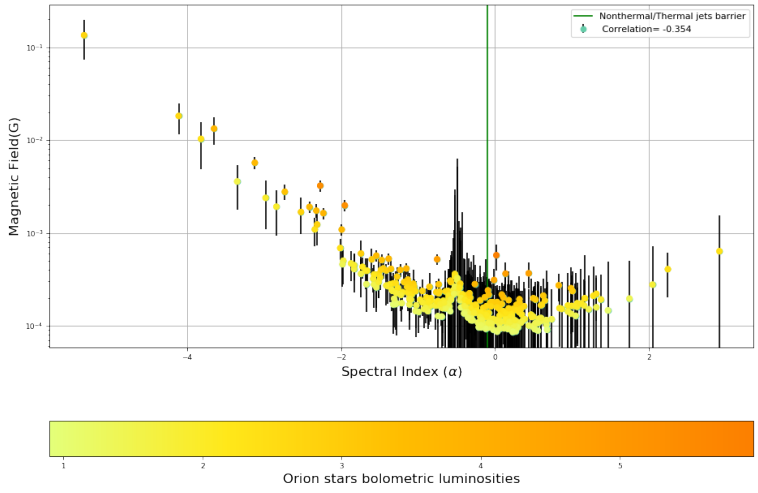

(a)

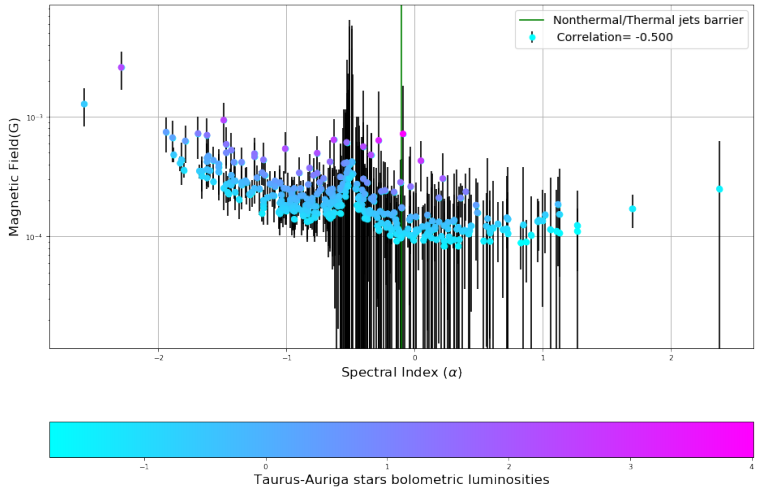

(b)

Figure 3: Magnetic field of Orion region sources (a) and Taurus-Auriga region sources (b) plotted as a function of the spectral index and color mapped with their bolometric luminosities

Figure 3 clearly shows difference in magnetic field values between non-thermal and thermal regimes. The range for the Orion source's spectral indices is $-6 \leq \alpha \leq 3$,extending much more than the Taurus-Auriga sources which is $-3 \leq \alpha \leq 2.5$. A spectral index of $\alpha \leq -2$ is not expected for a young stellar object, moreover the sources in the deep negative spectral index regime were unclassified by the Gould's catalog. I suggest that such objects may be AGN with high number of relativistic electrons, causing an unconventional power law.
The synchotron emission regime has a dominant magnetic field strength where it reaches a peak of 10^{-1}G . We can also see for non-thermal jets, as the spectral index increases, the magnetic field strength decreases. The decrease rate of the magnetic field is higher in range of $-6 \leq \alpha \leq -2$ and afterwards it continues the decline in a steady rate till it reaches 10^{-4}G.
Free-free emission regime magnetic field varies between 10^{-3}G and 10^{-4}G, where it slightly increase as the spectral index grow.

The more luminous objects are slightly above the average trend, the correlation coefficient (τ) for the Orion region is less than the Taurus-Auriga region by a relatively big margin. The correlations coefficients were τ= -0.354 and τ= -0.500 for Orion and Taurus-Auriga regions respectively. The correlations are lower than what we wanted since we expected a linear inverse relation as the spectral index increases indicating the absence of sychrotron radiation. However the magnetic field increases back again at $\alpha \approx 1.0$, and steadily rise in the free-free emission's regime. Another possibility for the correlation decrease is the the sudden jump in the magnetic field strength in both regions at $\alpha = -0.5$ mark. The error bars in this regime also rise which might justify the brief increase the magnetic field values to be an observational uncertainty. Though the Gould's Belt Survey did not mention any observational obstacles, having magnetic field values with errors up to one order of magnitude shows an increase in the flux density uncertainty.

Mukherjee et al. (2020) created different scenarios for low,medium and highly magnetized jets. For low magnetised jets $< 10^{-4}$G, they develop one of the MHD instabilities known as kink modes which is where most of the free-free emission thermal jets are, causing the cocoon to be asymmertic which can result in change in the direction of the outflow known as jet bending (Koide et al., 1996). Moreover, jets with magnetic field of $10^{-4}\text{G} < B < 10^{-3}$G classified as medium magnetised jets,exist in thermal and non-thermal jets develop small scale KH instabilities, intensifying as a result the interaction of the ionised outflow with the ambient medium round the cocoon. Sources with magnetic field $> 10^{-3}G$ are considered to be powerfully magnetised jets, prove to the most stable as they supress the instabilities using the resolving force of the toroidal component of the magnetic field. Those type of jets exist only in the negative spectral indices region, where there are 18 and 3 sources of them in Orion and Taurus-Auriga respectively.

4.2 Spectral index vs. Mass outflow rate

The mass outflow rate calculated for the sources in Figure 2 varied between $10^{-8}M_{\odot}\text{yr}^{-1}$ to $10^{-4}M_{\odot}\text{yr}^{-1}$. There has not been a clear relation between the type of jets and amount of mass lost in the ejection, however we see a different result in Figure 4.

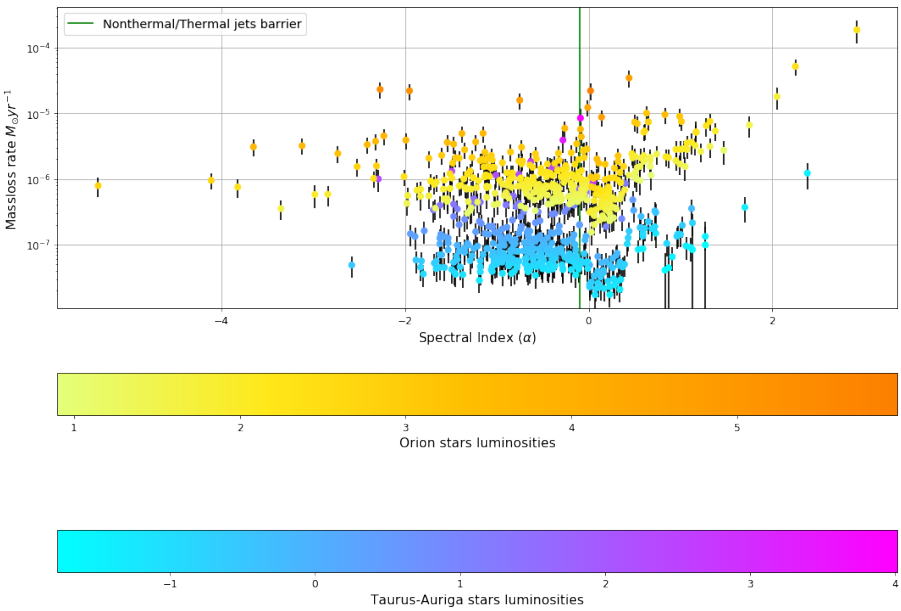

Figure 4: Sources color mapped by their luminosities and their mass outflow rate plotted as a function of the spectral index for both star formation regions

Firstly we see the clear distinction between the outflow rate when comparing the regions together. To understand the region comparison more clearly, we displayed the mass-loss comparison between both regions in Figure 8. Taurus-Auriga is a low-mass star formation region when compared to a more developed region with intermediate-high star formation, Orion in this case.
The ionised mass-loss rate for Orion region ranges between $10^{-6} M_\odot \mathrm{yr}^{-1}$ and $10^{-4} M_\odot \mathrm{yr}^{-1}$. For the Taurus-Auriga region, it ranges between around $10^{-8} M_\odot \mathrm{yr}^{-1}$ to $10^{-5} M_\odot \mathrm{yr}^{-1}$. We showed in Subsection 4.1 the high stability powerful magnetised jets have$> 10^{-3} G$, correspondingly the changes in mass-loss rates for the non-thermal jets occur only because of difference in envelope masses and as a result of the luminosities of the sources shown in the color map of Figure 4 (Duarte-Cabral, A. et al., 2013).

For thermal jets, a linear rise in the mass-loss rates to almost $10^{-4} M_\odot \mathrm{yr}^{-1}$ for the Orion region as the spectral index increase for Orion, however the rise in mass-loss rates for the Taurus-Auriga region is less significant as it increases to only $10^{-6} M_\odot \mathrm{yr}^{-1}$. We conclude that Orion region has heavier objects and stronger magnetic jets. To understand the relation between the mass-loss rate and the magnetic field in a more direct way, we present Figure 5

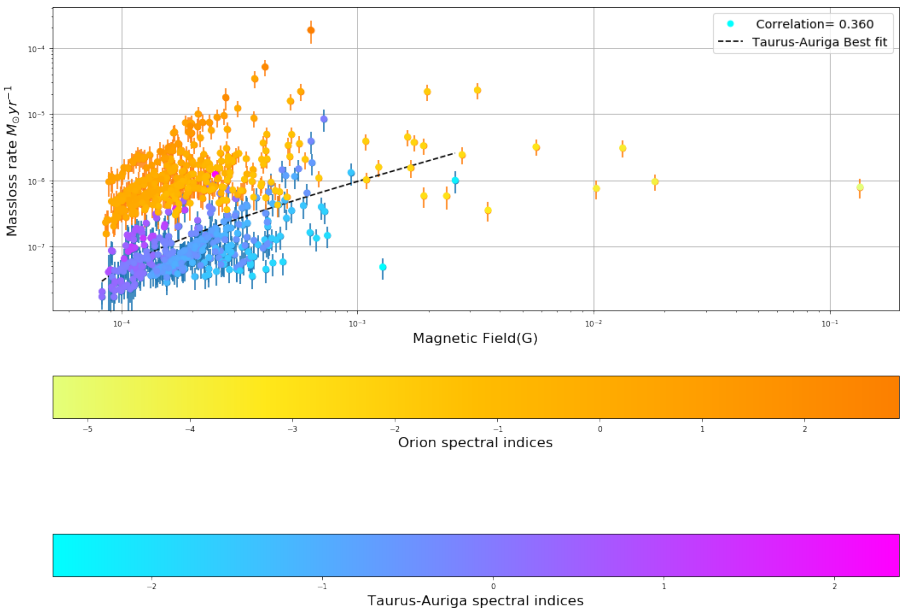

Figure 5: Sources color mapped by spectral index with their mass outflow rate plotted as a function of the magnetic field strength for both star formation regions

Highly magnetised jets($> 10^{-3}$G) do not have a specific relation with the amount of mass lost in the outflows. On the other hand, positive spectral indices grow stably with the mass-loss rate as the magnetic field increases from 10^{-4} to 10^{-3}G in both regions shown in Figure 5. A correlation to understand the relation between parameters was not possible for the Orion region as 18 sources with strongly magnetised jets extending to 10^{-1}G were present. The stability of these heavily magnetised jets do not cause the mass-loss outflow to differ, which affects the correlation of the relation. For the Taurus-Auriga region, only 3 sources had strong magnetic field strength, making it possible to calculate a correlation for the mass-loss outflow rate as a function of the magnetic field, acquiring a value of $\tau = 0.36$.

4.3 Bolometric Luminosity vs. Mass outflow rate

We expect a linear relation between the mass-loss rate in the outflows and the envelope mass as the heavier the accretion disk around the core is, the more material the object can eject in its outflows. Correspondingly, making the outflows more luminous(Bally, 2016).

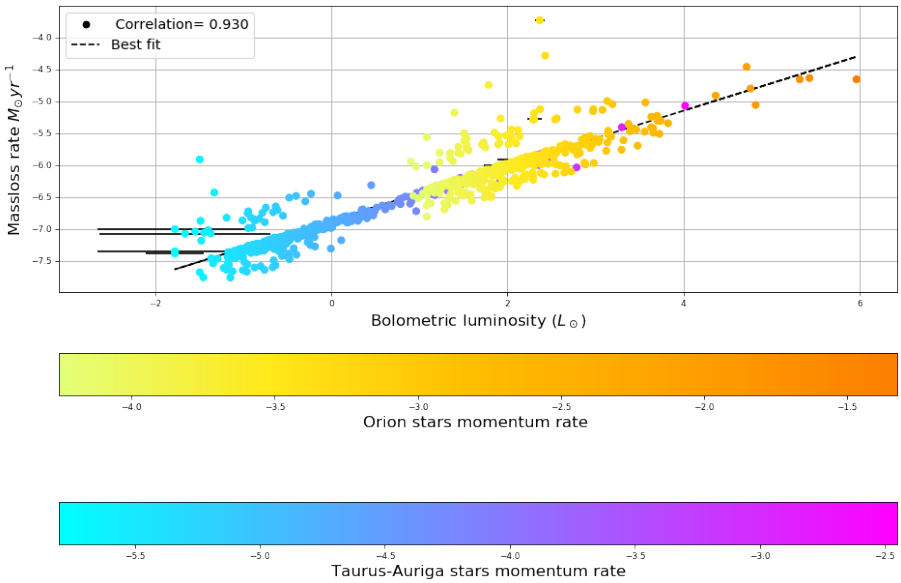

Figure 6: Mass-loss outflow rate plotted as a function of the bolometric luminosity, color mapped by the momentum rate in their outflows.

The mass-loss rate in the bipolar outflows increases in cohesion with the luminosity, showing the effect of having more mass around the clump to be accreted, resulting in a higher mass rate ejected by the helical magnetic field in the lobes (Beuther et al., 2002). Furthermore, the momentum flux rate in the outflows increase with the mass-loss rate, which is what we would expect as a result of the increasing mass of material in the outflows.

Moreover, we can also observe the massive unidentified objects around the region of Orion having luminosities of $10^4 \leq L_\odot \leq 10^6$, and the potential of having a black hole in the center of the region. The correlation coefficient for the plot is a notable τ=0.92 demonstrating the high dependence of mass-loss rate on envelope of the star with a p-value < 0.001.
We removed a total number of 44 sources from both regions due to high relative errors $\approx 80\%$ in the bolometric luminosity values due to the errors in the region distance and flux densities. The rise in errors for especially the Orion region could be because of their relative long distance of 414pc when compared to the Taurus-Auriga region at a distance of 137pc.

4.4 Momentum vs. Magnetic field

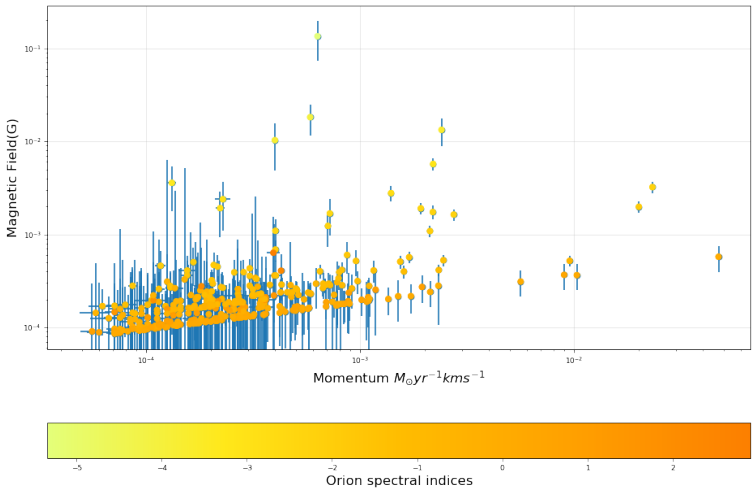

(a)

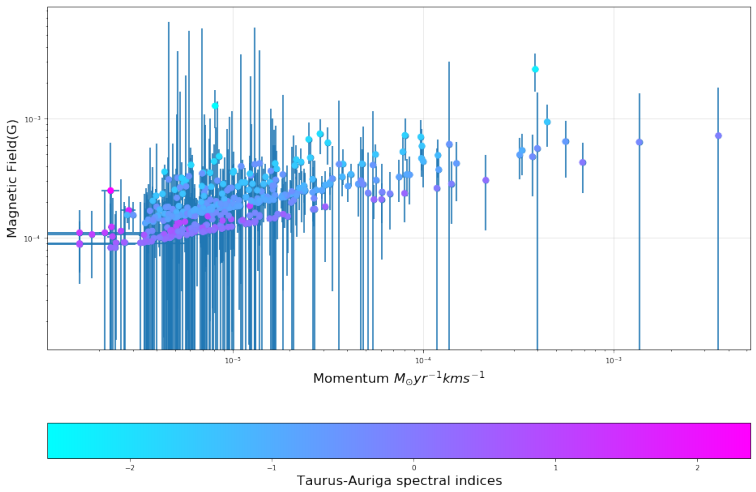

(b)

Figure 7: Sources mapped in their spectral indices with the magnetic field in the outflows plotted as a function of the momentum outflow rates for Orion(a) and Taurus-Auriga(b) regions

Figure 4 and Figure 5 demonstrated for us the non-linear relation the mass-loss rate have with the magnetic field. Moreover, it is shown in Figure 9 the randomness between the spectral index and momentum flux, therefore we did not expect a direct correlation between the momentum outflow rate and the magnetic field. For the Taurus-Auriga, the low-mass region has a correlation value of $\tau = 0.33$ with a p-value < 0.001. Demonstrating the weak relation between the momentum rate and poorly magnetised jets as the Taurus region only has 3 sources that are highly magnetised. On the other hand, Orion region has 18 sources that are highly magnetised jets, its momentum does not have a correlation with the magnetic field ($\tau < 0.017$). The momentum rate plotted in Figure 7 shows the dim relation with weak magnetised jets mostly found in the thermal jets regime but has zero correlation with high magnetised jets found at $\alpha < -2$.

5 Discussion

For 706 protostars in 2 star-forming regions, we have found a trend of synchotron emission mechanism with the magnetic field and how high ($> 10^{-1}$G) the magnetic field strength can get for negative spectral indices . In addition, we explained with the help of simulations how can powerful magnetised jets suppress the MHD instabilities, while moderate and low magnetised jets($< 10^{-3}$G) go through two types of MHD instabilities. Low magnetised jets can only be found in thermal jets. In this section we will discuss further research that could be done to add more to the results that could improve our understanding towards jets and their outflows.

5.1 Core mass calculation

Calculating the core mass of the sources will allow us to correlate it with the ionised mass-loss rates in the outflows. It was not possible with only Gould's Belt Survey measurements, as the survey focused on radiation emission at radio wavelengths. To be able to acquire the envelope's mass, we would need the flux density of interstellar dust at millimeter wavelengths (Hildebrand, 1983; Schuller et al., 2009). Moreover, we can also compare the sources core mass with molecular outflows, expecting a relation of $M_{out} \sim 0.1\ M_{core}^{0.8}$ where M_{core} is the core mass and M_{out} is the mass outflow in observed in CO. This relation was found through observing 26 massive young stars CO outflows (Bontemps, Andre, Terebey, & Cabrit, 1996; Cabrit & Bertout, 1992).
Furthermore, a classification for the sources in terms of their evolution could be obtained using their core masses and bolometric luminosities (Molinari et al., 2016). This could give us an overview on the difference ages of star formation regions and type of stars that exist there.

5.2 Jet velocities

An improvement that can be implemented, is measuring the jet velocities for all the sources that lie in the Taurus-Auriga and Orion regions. The measurement of the outflow velocities could be possible through observing the spectra for molecular and radio emission tracers (Arce et al., 2013). A more accurate mass-loss rate could be obtained using Equation 1 and as a result acquire a better relation between the core mass and the ejected ionised mass. We could also compare the velocity of molecular and ionised outflow of the same source, in order to find a link between the accelerated ambient medium and the ejected hot material in the outflows.

5.3 Polarized emission

Polarization make up 10% to 30% of the total synchotron radiation emission. Detecting polarized synchrotron emission may help us get a better approximation for the magnetic field direction in the jets. The degree of polarization in the jets can also tell us how effective is the magnetic field in large scales jets (Carrasco-Gonzalez et al., 2010; Pacholczyk, 1970).

With the Next Generation Very large Array(ngVLA) starting early science in 2028, it is considered to be 10 times more sensitive than the VLA, allowing us to process thermal and non-thermal line emission at a resolution of milliarcsecond (Ford et al., 2019). Additionally, the Square Kilometre Array(SKA) expected to operate around 2030, will operate at low radio frequencies ranging from 50MHz to 350MHz to perform interferometric imaging at a resolution of milli-arcsecond, in which one of its observing goals to setup a polarisation imaging pipeline with a noise-limited band (SKAO, 2015).

6 Conclusion

We confirmed the expectations of non-thermal jets having highly magnetised jets (Blandford & Payne, 1982; Carrasco-Gonzalez et al., 2010), where we assumed the equipartition function of energy to calculate the magnetic field strength. Non-thermal jets reached magnetic field values of 10^{-1}G while the thermal jets optically thick with free-free emission could only reach 10^{-3}G. Using the simulations of Mukherjee et al. (2020) helps us to illustrate the environment the magnetic field sets for the outflows. The kink modes and KH instabilities are present on different scales for low ($< 10^{-4}G$) and average ($10^{-4}\text{G} < B < 10^{-3}\text{G}$) magnetized jets, where thermal jets mostly experience these MHD instabilities.

The mass-loss calculation was mainly based on approximating the model of the jets and estimating the velocity of the ionised material. Figure 4 shows the stability of mass-loss rates for non-thermal jets because of the strong toroidal magnetic field component and demonstrates how the luminosity is the main parameter affecting its mass-loss rate in the outflows. Thermal jets mass-loss rates increase in an approximately linear relation with the spectral index.

The difference between the two regions we used in our research was noticeable in terms of momentum flux rate, mass-loss rate and bolometric luminosity. This allowed us to observe the difference in physical parameters between both regions. Subsection 4.2 showed how the mass-loss rates for the Orion region can go up to $10^{-4}M_{\odot}\text{yr}^{-1}$. It also had 168 sources that had mass-loss rates $> 10^{-6}M_{\odot}\text{yr}^{-1}$ while Taurus-Auriga region only had 10 sources with mass-loss rates $> 10^{-6}M_{\odot}\text{yr}^{-1}$. We deduced relations for the mass-loss rates and magnetic field with thermal and non-thermal jets, however we did not find a correlation between the momentum rate flux and the spectral indices of the jets as shown in Figure 9.

We also suggest parameters of interest for future studies. In order to relate the velocity and mass-loss rate of the hot ejected matter colliding with the shocked ambient medium, we would measure the spectra of molecular and ionised emission for the sources. Moreover, observing the dust emission of sources is essential for calculating the core mass of the YSOs. The upcoming generations of baseline arrays(SKA and ngVLA) have expectations in terms of providing reliable-high resolution data. This should further clarify the quantitative results we have regarding the magnetic field strength and mass-loss rates.

References

Anglada, G., Rodriguez, L. F., Canto, J., Estalella, R., & Torrelles, J. M. (1992, August). Radio Continuum from the Powering Sources of the RNO 43, Haro 4-255 FIR, B335, and PV Cephei Outflows and from the Herbig-Haro Object 32A. *apj*, *395*, 494. doi: 10.1086/171670

Anglada, G., Rodriguez, L. F., & Carrasco-Gonzalez, C. (2018, 11). Radio jets from young stellar objects. *The Astronomy and Astrophysics Review*, *26*, 3. Retrieved 2022-05-05, from https://arxiv.org/abs/1806.06444 doi: 10.1007/s00159-018-0107-z

Arce, H. G., Mardones, D., Corder, S. A., Garay, G., Noriega-Crespo, A., & Raga, A. C. (2013, September). ALMA Observations of the HH 46/47 Molecular Outflow. *apj*, *774*(1), 39. doi: 10.1088/0004-637X/774/1/39

Arce, H. G., Shepherd, D., Gueth, F., Lee, C. F., Bachiller, R., Rosen, A., & Beuther, H. (2007, January). Molecular Outflows in Low- and High-Mass Star-forming Regions. In B. Reipurth, D. Jewitt, & K. Keil (Eds.), *Protostars and planets v* (p. 245).

Bacciotti, F., Ray, T. P., Eislöffel, J., Woitas, J., Solf, J., Mundt, R., & Davis, C. J. (2003, January). Observations of Jet Diameter, Density and Dynamics. *apss*, *287*(1), 3-13. doi: 10.1023/B:ASTR.0000006192.17206.b5

Balbus, S. A., & Hawley, J. F. (1991, 07). A powerful local shear instability in weakly magnetized disks. i - linear analysis. ii - nonlinear evolution. *The Astrophysical Journal*, *376*, 214. doi: 10.1086/170270

Bally, J. (2016, 09). Protostellar outflows. *Annual Review of Astronomy and Astrophysics*, *54*, 491-528. doi: 10.1146/annurev-astro-081915-023341

Barsony, M. (1994, January). Class 0 Protostars. In D. P. Clemens & R. Barvainis (Eds.), *Clouds, cores, and low mass stars* (Vol. 65, p. 197).

Begelman, M. C. (1998, 01). Instability of toroidal magnetic field in jets and plerions. *The Astrophysical Journal*, *493*, 291-300. doi: 10.1086/305119

Beuther, H., Schilke, P., Sridharan, T. K., Menten, K. M., Walmsley, C. M., & Wyrowski, F. (2002, March). Massive molecular outflows. *aap*, *383*, 892-904. doi: 10.1051/0004-6361:20011808

Blandford, R. D., & Ostriker, J. P. (1978, 04). Particle acceleration by astrophysical shocks. *The Astrophysical Journal*, *221*, L29. doi: 10.1086/182658

Blandford, R. D., & Payne, D. G. (1982, 08). Hydromagnetic flows from accretion discs and the production of radio jets. *Monthly Notices of the Royal Astronomical Society*, *199*, 883-903. doi: 10.1093/mnras/199.4.883

Bontemps, S., Andre, P., Terebey, S., & Cabrit, S. (1996, July). Evolution of outflow activity around low-mass embedded young stellar objects. *aap*, *311*, 858-872.

Bordovitsyn, V. A., & Ternov, I. M. (1999). *Synchrotron radiation theory and its development : in memory of i.m. ternov*. World Scientific.

Cabrit, S., & Bertout, C. (1992, July). CO line formation in bipolar flows. III. The energetics of molecular flows and ionized winds. *aap*, *261*, 274-284.

Carrasco-Gonzalez, C., Rodriguez, L. F., Anglada, G., Marti, J., Torrelles, J. M., & Osorio, M. (2010, 11). A magnetized jet from a massive protostar. *Science*, *330*, 1209-1212. doi: 10.1126/science.1195589

Cohen, M., & Bieging, J. H. (1986, 12). Radio variability and structure of t tauri stars. *The Astronomical Journal*, *92*, 1396. doi: 10.1086/114273

Donati, J.-F., Paletou, F., Bouvier, J., & Ferreira, J. (2005, 11). Direct detection of a magnetic field in the innermost regions of an accretion disk. *Nature*, *438*, 466-469. doi: 10.1038/nature04253

Draine, B. T. (2011). *Physics of the interstellar and intergalactic medium*. Princeton University Press.

Duarte-Cabral, A., Bontemps, S., Motte, F., Hennemann, M., Schneider, N., & André, Ph. (2013). Co outflows from high-mass class 0 protostars in cygnus-x. *A&A*, *558*, A125. Retrieved from https://doi.org/10.1051/0004-6361/201321393 doi: 10.1051/0004-6361/201321393

Dunham, M. M., Allen, L. E., Evans, I., Neal J., Broekhoven-Fiene, H., Cieza, L. A., Di Francesco, J., ... Young, K. E. (2015, September). Young Stellar Objects in the Gould Belt. *apjs*, *220*(1), 11. doi: 10.1088/0067-0049/220/1/11

Dzib, Loinard, L., Mioduszewski, A. J., Boden, A. F., Rodríguez, L. F., & Torres, R. M. (2010, 07). Vlba determination of the distance to nearby star-forming regions. iv. a preliminary distance to the proto-herbig aebe star ec 95 in the serpens core. *The Astrophysical Journal*, *718*, 610-619. doi: 10.1088/0004-637x/718/2/610

Dzib, Loinard, L., Mioduszewski, A. J., Rodríguez, L. F., Ortiz-León, G. N., Pech, G., ... Tobin, J. (2013, sep). THE GOULD's BELT VERY LARGE ARRAY SURVEY. i. THE OPHIUCHUS COMPLEX. *The Astrophysical Journal*, *775*(1), 63. Retrieved from https://doi.org/10.1088/0004-637x/775/1/63 doi: 10.1088/0004-637x/775/1/63

Dzib, S. A., Loinard, L., Rodríguez, L. F., Mioduszewski, A. J., Ortiz-León, G. N., Kounkel, M. A., ... Tobin, J. (2015, 03). The gould's belt very large array survey. iv. the taurus-auriga complex. *The Astrophysical Journal*, *801*, 91. doi: 10.1088/0004-637x/801/2/91

Elmegreen, B. G., & Scalo, J. (2004, September). Interstellar Turbulence I: Observations and Processes. *araa*, *42*(1), 211-273. doi: 10.1146/annurev.astro.41.011802.094859

Feigelson, E. D., & Montmerle, T. (1985, 02). An extremely variable radio star in the rho ophiuchi cloud. *The Astrophysical Journal*, *289*, L19. doi: 10.1086/184426

Ford, E., Cole, G., Ball, L., Butler, B., Durand, B. C. S., Erickson, A., ... Wrobel, J. (2019). *Operations concept.* Retrieved 2022-07-05, from https://ngvla.nrao.edu/download/MediaFile/231/original

Hawley, J., Fendt, C., Hardcastle, M., Nokhrina, E., & Tchekhovskoy, A. (2015, 08). Disks and jets - gravity, rotation and magnetic fields. *Space Science Reviews*, *191*. doi: 10.1007/s11214-015-0174-7

Hildebrand, R. (1983, 09). The determination of cloud masses and dust characteristics from submillimetre thermal emission. *Quarterly Journal of the Royal Astronomical Society*, *24*, 267-282.

Kavak, Sánchez-Monge, Á., López-Sepulcre, A., Cesaroni, R., van der Tak, F. F. S., Moscadelli, L., ... Schilke, P. (2021). Search for radio jets from massive young stellar objects - association of radio jets with h2o and ch3oh masers. *A&A*, *645*, A29. Retrieved from https://doi.org/10.1051/0004-6361/202037652 doi: 10.1051/0004-6361/202037652

Kee, N. D., Owocki, S., & Sundqvist, J. O. (2016, 03). Line-driven ablation of circumstellar discs – i. optically thin decretion discs of classical oe/be stars. *Monthly Notices of the Royal Astronomical Society*, *458*, 2323-2335. doi: 10.1093/mnras/stw471

Kigure, H., & Shibata, K. (2005, 12). Three-dimensional magnetohydrodynamic simulations of jets from accretion disks. *The Astrophysical Journal*, *634*, 879-900. doi: 10.1086/497130

Koide, S., Sakai, J.-I., Nishikawa, K.-I., & Mutel, R. L. (1996, 06). Numerical simulation of bent jets: Propogation into an oblique magnetic field. *The Astrophysical Journal*, *464*, 724. doi: 10.1086/177359

Kounkel, M., Hartmann, L., Loinard, L., Mioduszewski, A. J., Dzib, S. A., Ortiz-León, G. N., ... Tobin, J. (2014, 07). The gould's belt very large array survey. iii. the orion region. *The Astrophysical Journal*, *790*, 49. doi: 10.1088/0004-637x/790/1/49

Lada, C. J. (1985, 09). Cold outflows, energetic winds, and enigmatic jets around young stellar objects. *Annual Review of Astronomy and Astrophysics*, *23*, 267-317. doi: 10.1146/annurev.aa.23.090185.001411

Menten, K. M., Reid, M. J., Forbrich, J., & Brunthaler, A. (2007). The distance to the orion nebula. *A&A*, *474*(2), 515-520. Retrieved from https://doi.org/10.1051/0004-6361:20078247 doi: 10.1051/0004-6361:20078247

Miley, G. (1980, 09). The structure of extended extragalactic radio sources. *Annual Review of Astronomy and Astrophysics*, *18*, 165-218. doi: 10.1146/annurev.aa.18.090180.001121

Mohan, S., Vig, S., & Mandal, S. (2022, 05). Radio spectra of protostellar jets: Thermal and non-thermal emission. *Monthly Notices of the Royal Astronomical Society*. doi: 10.1093/mnras/stac1159

Molinari, S., Merello, M., Elia, D., Cesaroni, R., Testi, L., & Robitaille, T. (2016, jul). CALIBRATION OF EVOLUTIONARY DIAGNOSTICS IN HIGH-MASS STAR FORMATION. *The Astrophysical Journal*, *826*(1), L8. Retrieved from https://doi.org/10.3847/2041-8205/826/1/l8 doi: 10.3847/2041-8205/826/1/l8

Motte, F., Bontemps, S., & Louvet, F. (2018). High-mass star and massive cluster formation in the milky way. *Annual Review of Astronomy and Astrophysics*, *56*(1), 41-82. Retrieved from https://doi.org/10.1146/annurev-astro-091916-055235 doi: 10.1146/annurev-astro-091916-055235

Mukherjee, D., Bodo, G., Mignone, A., Rossi, P., & Vaidya, B. (2020, 09). Simulating the dynamics and non-thermal emission of relativistic magnetized jets i. dynamics. *Monthly Notices of the Royal Astronomical Society*, *499*, 681-701. doi: 10.1093/mnras/staa2934

Obonyo, W. O., Lumsden, S. L., Hoare, M. G., Purser, S. J. D., Kurtz, S. E., & Johnston, K. G. (2019, 04). A search for non-thermal radio emission from jets of massive young stellar objects. *Monthly Notices of the Royal Astronomical Society*, *486*, 3664-3684. doi: 10.1093/mnras/stz1091

Ortiz-Leó n, G. N., Loinard, L., Mioduszewski, A. J., Dzib, S. A., Rodríguez, L. F., Pech, G., ... González-Lópezlira, R. A. (2015, may). THE GOULD's BELT VERY LARGE ARRAY SURVEY. II. THE SERPENS REGION. *The Astrophysical Journal*, *805*(1), 9. Retrieved from https://doi.org/10.1088%2F0004-637x%2F805%2F1%2F9 doi: 10.1088/0004-637x/805/1/9

Pacholczyk, A. G. (1970). *Radio astrophysics. Nonthermal processes in galactic and extragalactic sources.*

Pudritz, R. E., & Norman, C. A. (1983, 11). Centrifugally driven winds from contracting molecular disks. *The Astrophysical Journal*, *274*, 677. doi: 10.1086/161481

Pudritz, R. E., Ouyed, R., Fendt, C., & Brandenburg, A. (2006). *Disk winds, jets, and outflows: Theoretical and computational foundations.* arXiv. Retrieved from https://arxiv.org/abs/astro-ph/0603592 doi: 10.48550/ARXIV.ASTRO-PH/0603592

Purser, S. J. D., Lumsden, S. L., Hoare, M. G., & Kurtz, S. (2021, 03). A galactic survey of radio jets from massive protostars. *Monthly Notices of the Royal Astronomical Society*, *504*, 338-355. doi: 10.1093/mnras/stab747

Purser, S. J. D., Lumsden, S. L., Hoare, M. G., Urquhart, J. S., Cunningham, N., Purcell, C. R., ... Voronkov, M. A. (2016, 05). A search for ionized jets towards massive young stellar objects. *Monthly Notices of the Royal Astronomical Society*, *460*, 1039-1053. doi: 10.1093/mnras/stw1027

Reid, M. J., Argon, A. L., Masson, C. R., Menten, K. M., & Moran, J. M. (1995, April). Synchrotron Emission from the H 2O Maser Source in W3(OH). *apj*, *443*, 238. doi: 10.1086/175518

Reipurth, B., & Bally, J. (2001, January). Herbig-Haro Flows: Probes of Early Stellar Evolution. *araa*, *39*, 403-455. doi: 10.1146/annurev.astro.39.1.403

Reynolds, S. P. (1986, 05). Continuum spectra of collimated, ionized stellar winds. *The Astrophysical Journal*, *304*, 713. Retrieved 2022-05-18, from https://articles.adsabs.harvard.edu/

pdf/1986ApJ...304..713R doi: 10.1086/164209

Rodriguez, L. F., Curiel, S., Moran, J. M., Mirabel, I. F., Roth, M., & Garay, G. (1989, 11). Large proper motions in the remarkable triple radio source in serpens. *The Astrophysical Journal*, *346*, L85. doi: 10.1086/185585

Rodriguez, L. F., Moran, J. M., Gottlieb, E. W., & Ho, P. T. P. (1980, 02). Radio observations of water vapor, hydroxyl, silicon monoxide, ammonia, carbon monoxide, and compact h ii regions in the vicinities of suspected herbig-haro objects. *The Astrophysical Journal*, *235*, 845. doi: 10.1086/157687

Rodríguez-Kamenetzky, A., Carrasco-González, C., Torrelles, J. M., Vlemmings, W. H. T., Rodríguez, L. F., Surcis, G., ... van Langevelde, H. J. (2020, 06). Characterizing the radio continuum nature of sources in the massive star-forming region w75n (b). *Monthly Notices of the Royal Astronomical Society*, *496*, 3128-3141. doi: 10.1093/mnras/staa1742

Sanna, A., Moscadelli, L., Cesaroni, R., Caratti o Garatti, A., Goddi, C., & Carrasco-González, C. (2016, 11). Momentum-driven outflow emission from an o-type yso. *Astronomy and Astrophysics*, *596*, L2. doi: 10.1051/0004-6361/201629544

Schuller, F., Menten, K. M., Contreras, Y., Wyrowski, F., Schilke, P., Bronfman, L., ... Weiß, A. (2009, 05). Atlasgal – the apex telescope large area survey of the galaxy at 870 μm. *Astronomy and Astrophysics*, *504*, 415-427. doi: 10.1051/0004-6361/200811568

Schwartz, R. D. (1983, 09). Herbig-haro objects. *Annual Review of Astronomy and Astrophysics*, *21*, 209-237. doi: 10.1146/annurev.aa.21.090183.001233

Shu, F. H., Adams, F. C., & Lizano, S. (1987, 09). Star formation in molecular clouds: Observation and theory. *Annual Review of Astronomy and Astrophysics*, *25*, 23-81. doi: 10.1146/annurev.aa.25.090187.000323

SKAO. (2015). *Ska1 observing bands: Scientific context.* Retrieved 2022-07-05, from https://www.skao.int/sites/default/files/documents/d5-SKA1-Observing-Bands-V3a_0.pdf

Tan, J. C., Beltrá n, M. T., Caselli, P., Fontani, F., Fuente, A., Krumholz, M. R., ... Stolte, A. (2014). Massive star formation. In *Protostars and planets VI.* University of Arizona Press. Retrieved from https://doi.org/10.2458%2Fazu_uapress_9780816531240-ch007 doi: 10.2458/azu_uapress_9780816531240-ch007

Torres, R. M., Loinard, L., Mioduszewski, A. J., & Rodriguez, L. F. (2007, dec). VLBA determination of the distance to nearby star-forming regions. II. hubble 4 and HDE 283572 in taurus. *The Astrophysical Journal*, *671*(2), 1813–1819. Retrieved from https://doi.org/10.1086/522924 doi: 10.1086/522924

Vig, S., Veena, V. S., Mandal, S., Tej, A., & Ghosh, S. K. (2017, 11). Detection of non-thermal emission from the massive protostellar jet hh80-81 at low radio frequencies using gmrt. *Monthly Notices of the Royal Astronomical Society*, *474*, 3808-3816. doi: 10.1093/mnras/stx3032

7 Appendices

A: Mass-loss outflow rate distribution

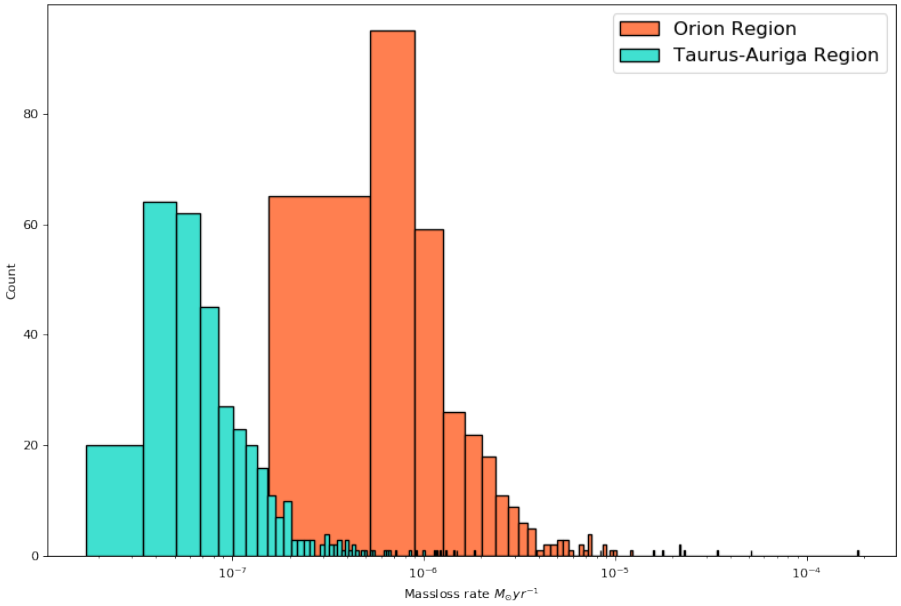

Figure 8: Distribution of the mass-loss rate for Taurus-Auriga and Orion regions

B: Spectral index vs. Momentum flux rate

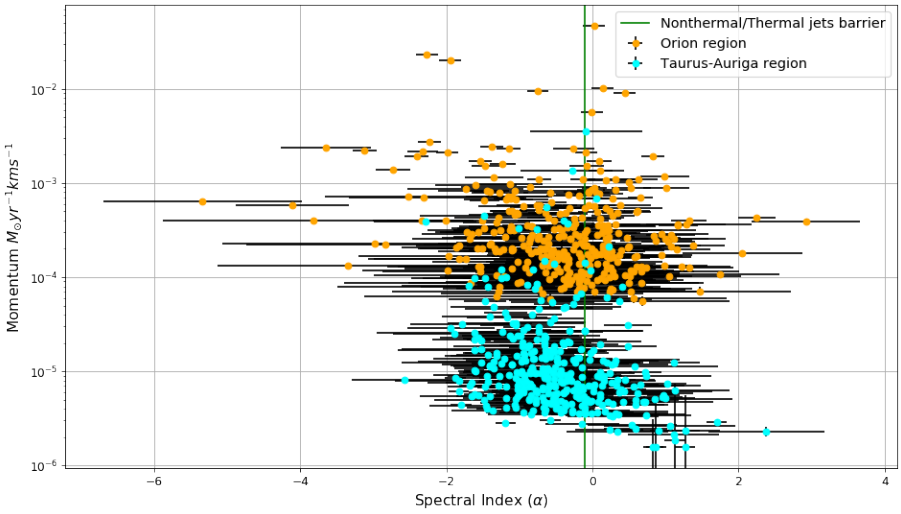

Figure 9: The spectral index of the sources plotted with the momentum rate flux in the outflows.